特　集　**磁気軸受**

An AMB Energy Storage Flywheel for Industrial Applications

Larry Hawkins[1] and Pat McMullen[2]
[1]Calnetix, Inc., Cerritos, California, USA
[2]Vycon, Inc., Yorba Linda, California, USA

The characteristics of an active magnetic bearing (AMB) supported energy storage flywheel are discussed. The flywheel was developed for a number of industrial applications to provide: 1) ride-through power in turbine or diesel generator sets, 2) voltage support in rail applications, 3) energy recovery in crane applications, 4) power quality improvement, and 5) load support in uninterruptible power supplies (UPS). The flywheel system operates in a vacuum to minimize windage losses, uses AMB to minimize bearing losses and eliminate bearing maintenance, and has a high power motor/generator coupled to an efficient power conversion module. The magnetic bearing system is designed to minimize losses for both energy storage efficiency and to reduce heat generated on the rotating assembly. The magnetic bearing controller uses synchronous cancellation to minimize dynamic loads (and losses). This is demonstrated by dynamic data from high speed testing. Rotor temperature measurements from thermal equilibrium testing are also presented.

Keywords: energy storage flywheel, magnetic bearings, UPS.

1. BACKGROUND

A flywheel energy storage system has been developed for industrial applications. The flywheel based storage system is targeted for some applications where the characteristics of flywheels offer advantages over chemical batteries: 1) ride-through power in turbine or diesel generator sets, 2) voltage support in rail applications, 3) power quality improvement, and 4) uninterruptible power supplies (UPS). Some of the key advantages offered by flywheels compared to batteries are: 1) known energy ready status, 2) life is unaffected by high discharge and charge rates, 3) no routine maintenance is required, 4) they are relatively insensitive to high ambient temperatures, 5) less floor space is required and power density is higher for flywheels, and 6) they have none of the environmental concerns with eventual disposal that arise with lead-acid batteries.

Flywheel based systems are particularly advantageous in UPS systems when combined with diesel or turbine generator sets (gensets). In order to protect against prolonged outages, mission critical applications often require the installation of gensets to ensure continuous operation once the typical 10-minute battery life is exhausted. With 90% of all power quality events lasting less than 3 seconds and the ones lasting more than 3 seconds almost always causing outages lasting in hours rather than minutes, flywheel based UPS systems make sense for the entire spectrum of power quality events. Energy stored in the flywheel is used for events lasting less than 3 seconds. For longer events, the flywheel supplies ride-through power for the next 7 to 12 seconds while the genset is being brought on line to provide long-term power.

The ability of flywheel systems to quickly charge and discharge is a key enabling technology for applications requiring pulse power. One such application is the charging of the flywheel through the energy dissipated in the deceleration of a cargo container as it is being lowered by a gantry crane and discharging the captured energy in the acceleration of the container as it is subsequently lifted. This energy conservation allows for fuel savings from the on-board genset, thus reducing operating costs. Another similar application is the charging of the flywheel through the energy dissipated in the deceleration of a railway car and discharging the captured energy in the acceleration of the car. Traditional chemical batteries cannot be used in these applications due to the lapse in first charging the batteries (chemical reaction delays) and then discharging the batteries, once again chemical reaction delays. Additionally, this type of high frequency service severely reduces battery life, but has no exacerbating effect on flywheel life.

The flywheel system consists of two major subsystems: 1) the flywheel module, which includes the flywheel, motor/generator, and a five axis active magnetic bearing system, and 2) a three-phase bi-directional IGBT bridge (converter) used for both motoring and generation. The output and input to the flywheel system is through a DC bus into and out of the converter. The converter creates a sine wave drive from the DC bus to drive the flywheel during motoring, and converts the varying sinusoidal frequency and voltage from the flywheel to DC during generation. Details of the converter were reported in [1]. The design of the flywheel module is reported here.

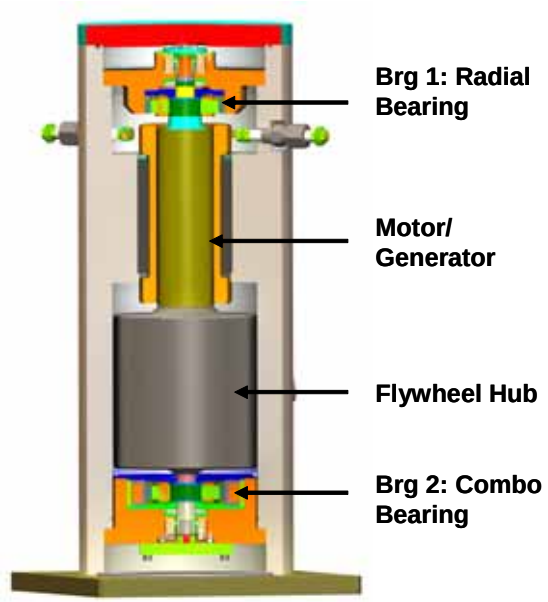

Fig. 1 The energy storage flywheel.

The flywheel module, shown in Fig. 1, is designed to store a total of 1.25 kWh at 36,000 rpm and deliver 160kW (200 kVA) for more than 18 seconds, or 300kw for 5 seconds. In many flywheel designs that have been suggested, the goal of maximizing energy density has lead to carbon fiber composites as the material choice for the flywheel hub. This can result in an expensive design, and some difficult design tradeoffs. A key design goal for this industrial flywheel was to keep the cost for the flywheel system low with the same peak power of an equivalent battery system. This goal leads to high strength steel as the material of choice for the flywheel hub. To maximize efficiency, the flywheel rotor operates in a vacuum and uses magnetic bearings. Thus rotor heat removal must be accomplished through radiation, making minimization of rotor heating a major design consideration. Consequently, low-loss homopolar, permanent magnet bias magnetic bearings and a permanent magnet motor/generator were chosen to reduce rotor heating. Thermal testing is now underway and initial results are reported here.

2. ENERGY STORAGE FLYWHEEL

The vertically mounted flywheel (Fig. 1) uses a steel flywheel placed below a separate motor/generator on the same shaft. This partially integrated configuration was chosen to allow integration of an existing, proven motor/generator with a robust flywheel design. Similar configurations have been well tested and proven to be reliable [2],[3],[4]. Although the flywheel hub has a fairly high Ip/It, the rigid body Ip/It for the entire flywheel rotor is quite low (0.25) due to the size of the high-power density motor/generator. This feature helps to simplify the magnetic bearing control. The motor/generator utilizes a two-pole permanent magnet rotor designed by Calnetix Inc. The magnet is captured radially by a thick non-magnetic sleeve, which also provides the structural connection to the rest of the flywheel rotor. The magnetic bearings are placed immediately above the motor/generator and immediately below the flywheel. Rolling element backup bearings are placed outboard of the magnetic bearings.

2.1 Motor/Generator

The flywheel motor/generator incorporates a radially polarized permanent magnet (PM). PM machines use permanent magnets to provide field excitation, providing high efficiency and reduced size for an equivalent power when compared with other types of machines such as induction and switched reluctance machines. The motor/generator consists of a rotor assembly and a stator assembly. The rotor assembly contains the permanent magnets, which are constrained by a high strength steel retaining sleeve. The sleeve also provides the structural connection between the flywheel and the upper bearing shaft. The three-phase stator is conventionally wound, allowing a simple low cost construction. To ensure effective operation in the vacuum environment, the motor/generator design was optimized to minimize rotor losses due to tooth ripple effects and armature current harmonics.

2.2 Magnetic Bearing

The magnetic bearings use a homopolar, permanent magnet bias topology. Homopolar refers to the direction of the bias flux, which is oriented either uniformly into or uniformly out of the shaft at any circumferential location. This topology significantly reduces rotor eddy current losses compared to conventional designs. A permanent magnet is used to produce the bias flux for the bearing,

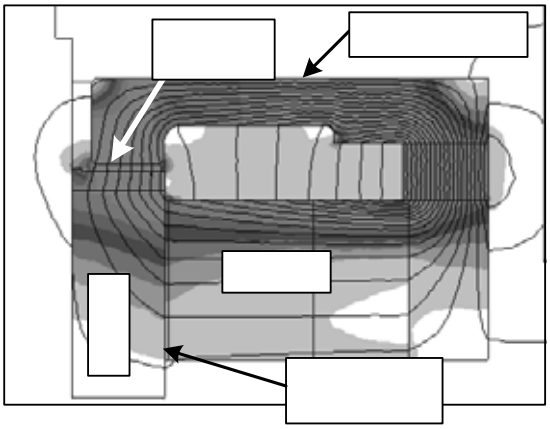

Fig. 2 Bias flux distribution in radial bearing with passive axial lift.

resulting in several advantages compared to electromagnetic bias: 1) less power is consumed by the magnetic bearings and 2) the bearing has a more linear force/displacement characteristic due to the contribution of the large, fixed reluctance of the permanent magnet to the bias flux path.

The radial bearing (Brg 1) has two radial control axes and a passive axial lift function. The axial lift is accomplished by returning the permanent magnet bias field through an upper side axial pole face of the rotor. The mechanism is clearly demonstrated in the magnetic finite element analysis result of Fig. 2 This passive axial axis of this bearing provides a passive vertical lift force of 500 N (112 lbf) at nominal air gap. A large air gap, 2.0 mm (0.079 in), limits the additional axial negative stiffness to 358,000 N/m (2,000 lb/in) making the passive lift force relatively insensitive to thermal or centrifugal changes in rotor length.

The combination (combo) bearing (Brg 2) in Fig. 1 is a three-axis combination radial/thrust bearing. The basic operation of this bearing topology was described in [5]. A combo bearing is more compact axially than separate radial and axial magnetic bearings. This increases the frequency of the rotor bending modes, making the magnetic bearing control design less difficult. Also, the passive lift feature of the radial bearing supports part of the rotor weight, reducing the required load capacity for the thrust axis of the combo bearing. The combo bearing uses a single radially polarized permanent magnet ring to provide bias flux for both the radial and axial flux paths. Three separate pairs of control coils allow individual control of each axis (two radial and one axial).

Some characteristics of the magnetic bearings are given in Table 1.

2.3 Backup Bearings

The backup bearings have radial and axial clearances of 0.18 mm (0.007 in) between the bearing inner races and the shaft. This clearance is less than one-half of the magnetic air gap. The backup bearings are expected to carry load in the following cases: 1) when the system is at rest and the magnetic bearings are turned off, 2) in the event of a substantial shock transient that exceeds the capacity of the magnetic bearings, and 3) in the event of a component failure that causes the loss of one more axes of control for the magnetic bearing.

Table 1**:** Magnetic bearing characteristics.

Bearing	**Radial Bearing**	**Combo Radial**	**Combo Axial**	**Passive Axial**
Bearing Reference Name	Brg 1	Brg 2	Axial	Axial
Coordinate Names	x1,y1	x2,y2	z	z1
Load Capacity, N (lbf)	555 (125)	555 (125)	1100 (250)	625 (140)
Force Constant, N/A (lbf/A)	77 (17.3)	77 (17.3)	279 (62.7)	-
Negative Stiffness, N/mm (lbf/in)	1050 (6,000)	1050 (6,000)	875 (5,000)	525 (3,000)
Air Gap, mm (in)	0.508 (.020)	0.508 (.020)	0.762 (.030)	1.016 (.040)
Maximum Current, A	7.2	7.2	4.0	-

The backup bearing system consists of a duplex pair of 25 mm angular contact ball bearings at each end of the shaft. The lower backup bearing also acts as a backup thrust bearing due to the inclusion of thrust collars on the rotor. The bearings are hybrid style with 52100 races and SiN_3 balls and a light fill of vacuum compatible grease. Steel sleeves are used for the rotor contacting surfaces. Radial flexibility is provided by an elastomeric element between the mount and housing. The mount is free to slide in an axial clearance space of 0.025 mm. The net radial stiffness is 5.0×10^6 N/m, resulting in a lowest radial natural frequency of 40 Hz. A hard stop limits radial deflection on the elastomer to 0.075 mm.

The backup bearing system has undergone extensive testing, including 46 full spin down drop tests on multiple units, and over 200 drops in different parts of the speed range. Initially, testing was done with accelerated spin downs – where the rotor speed was pulled down to zero in about 2 minutes using the generator. In subsequent test runs, this time was gradually extended until the rotor was COASTING down unassisted in approximately 2.75 hours. The tests were planned to evaluate a number of characteristics: 1) rotordynamic performance on the backup bearings, 2) bearing life, 3) rotor sleeve material, and 4) rotor thrust washer material. Backup bearing development and testing for this flywheel were reported extensively in [6].

A bronze touchdown sleeve was used during initial testing and worked well until spin down times were extended to about an hour. With longer spin down times, the bronze sleeve tended to expand enough through heating and rolling pressure to become loose on the shaft. A 4340 steel sleeve was then tested and performed well through all subsequent testing. The rotor thrust washer is subject to sliding friction with the backup bearing inner race as the rotor whirls at the 40 Hz whirl frequency. A bronze thrust washer was used initially, but it consistently wore approximately 0.05 mm during a thirty minute spin down. Several different materials and coatings were tested, and of those, the one with the lowest coefficient of friction (in vacuum) gave the best performance, lasting through six 2.75 hour spin downs with less than 0.025 mm total wear. In the testing performed to date, the life of the bearing itself has not been a limiting factor.

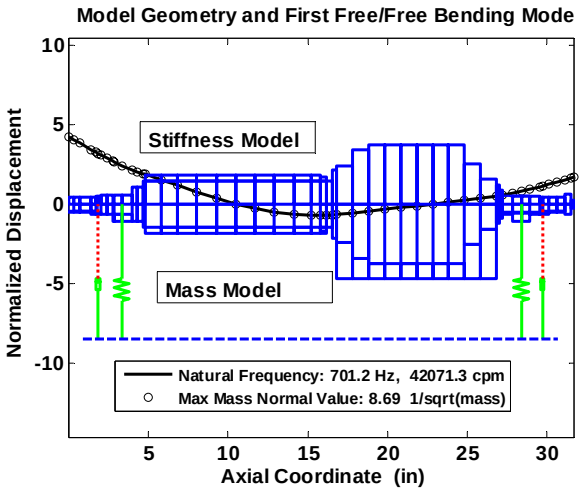

Fig. 3 Rotor model geometry and first bending mode.

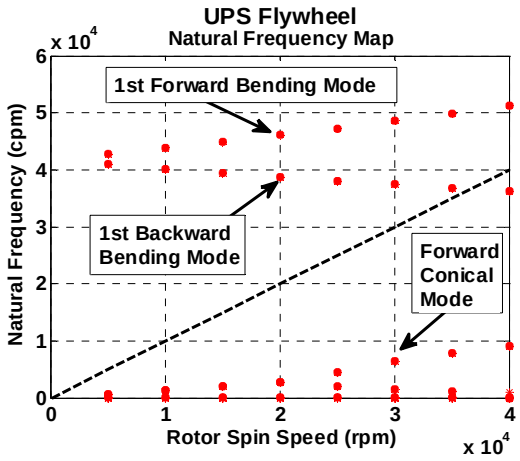

Fig. 4 Rotor free/free natural frequency map.

3. SYSTEM DYNAMIC CHARACTERISTICS

3.1 Rotordynamic Model

The rotordynamic structural model is shown in Fig. 3 The top half shows the stiffness model and the lower half the mass model. The actuator and sensor locations and the first free/free, zero-speed bending mode are superimposed on the plot. The first three bending modes are included in the system analysis. The frequencies of those modes at zero speed are: 701 Hz, 1415 Hz, and 1890 Hz.

The rotordynamic equation of motion for the plant, which is in general a coupled, flexible rotor/casing system with conventional bearings, is:

$$[M]\{\ddot{q}\}+[C]\{\dot{q}\}+[K]\{q\}=\{f\} \qquad \textbf{(1)}$$

Where q represents the physical coordinate degrees of freedom, f represents external forces, and the mass matrix is represented by **M**. The passive negative stiffness of the magnetic bearing is included in the bearing stiffness matrix, **K**. The terms representing gyroscopic effects are part of the rotor partition of the damping matrix, **C**. For the flywheel, each rotor bending mode was given a static internal damping ratio of 0.25%. This is a conservative value for a rotor with sleeves if no modal test data is available.

For system analysis with magnetic bearings, the plant represented by Eqn. (1) is transformed to modal coordinates, μ, and converted to state space form:

$$\begin{aligned}\{\dot{\mu}_P\}&=[A_P]\{\mu_P\}+[B_P]\{f\}\\ \{q\}&=[C_P]\{\mu_P\}+[D_P]\{f\}\end{aligned} \qquad \textbf{(2)}$$

Partitions of the characteristic matrix $\mathbf{A_P}$ contain the modal stiffness and damping matrices. The input and output matrices $\mathbf{B_P}$ and $\mathbf{C_P}$ contain mass normalized eigenvectors for modes selected for the system analysis. Some authors include the passive negative stiffness as part of the feed forward matrix $\mathbf{D_P}$ instead of as a bearing stiffness in **K**. These equations have been presented in detail by several authors; one recent example is Antkowiak [7].

A free/free plant natural frequency map is shown in Fig. 4 The forward conical rigid body mode, ω_n increases approximately with $\omega_n = Ip/It * \omega_s = 0.25 * \omega_s$. This relatively small change with speed is a convenient characteristic that somewhat simplifies the magnetic bearing control scheme. The first bending mode, however, is quite gyroscopic because the flywheel hub, which has most of the polar inertia of the rotating assembly, must continually change its angular momentum vector to execute the mode.

3.2 Basic Magnetic Bearing Compensator

Two different control schemes, both successful, have been used for the control compensation of the AMB. Initial spin testing and backup bearing drop testing is conducted using a very powerful prototype magnetic bearing controller (MBC). With this hardware, a single-input, single-output (SISO) compensator is used together with gain scheduling to provide stability throughout the operating speed range of the flywheel [3]. The prototype controller is used for initial testing because it has a large number of features for data acquisition and it has powerful current amplifiers that allow the rotor to be re-levitated in the middle of a backup bearing drop test when desired. The basic SISO magnetic bearing transfer function is shown for Brg 1 (x1 and y1) is given in Fig. 5 The transfer function for Brg 2 is similar.

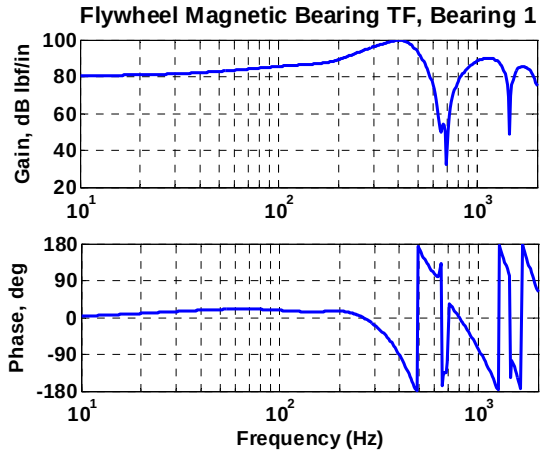

Fig. 5 Magnetic bearing force/displacement transfer function for Bearing 1.

For production units, an MBC is used that has been optimized for low cost and has an extensive reliability record. This MBC does not allow gain scheduling but does allow control using center-of-gravity (COG) coordinates (also called tilt/translation). With COG control, gain scheduling is unnecessary due to the relatively low rigid body *Ip/It* ratio of this flywheel. Both the COG compensation and the gain-scheduled SISO compensation have been shown to be robust and reliable in long term operation.

3.3 Adaptive Vibration Control

A key feature of any magnetic bearing controller is adaptive vibration control. There are numerous possible approaches that have been described in the literature, each with particular applications. The choice depends on the system requirements and what is to be accomplished. The approach most often described in the literature adaptively minimizes synchronous displacement using a learned gain matrix that represents the force/displacement influence coefficients of the system [8]. This approach is referred to in the ISO 14839-1 standard on magnetic bearings as Unbalance Force Counteracting Control (UFCC). A second approach adaptively minimizes synchronous current using a learned sensitivity matrix [9]. This approach is referred to in ISO 14839-1 as Unbalance Force Rejection Control (UFRC). Because UFRC minimizes synchronous current, it also minimized reaction force, housing vibration, and power consumption. This approach makes the most sense for flywheel energy storage systems. UFRC can be used from very low spin speeds, through the rigid body mode traverse, and up to close proximity of the first forward rotor bending mode. At higher speeds, well above the rigid body modes, UFRC is similar to adaptively minimizing the synchronous component of the error signal to the DSP, thereby reducing synchronous current.

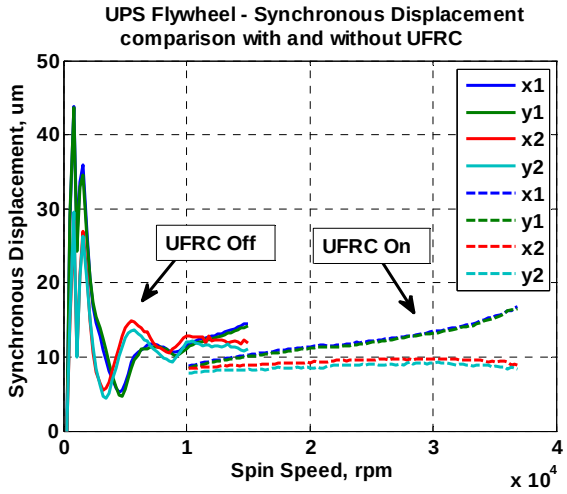

Fig. 6 Comparison of synchronous displacements with and without UFRC.

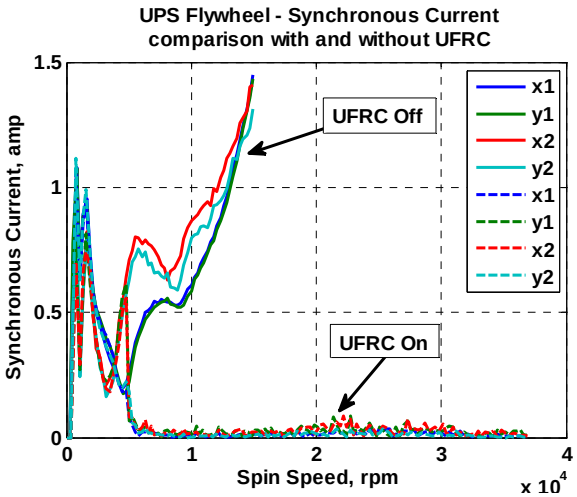

Fig. 7 Comparison of synchronous currents with and without UFRC.

4. SYNCHRONOUS RESPONSE MEASUREMENTS

Fig. 6 and Fig. 7 show dynamic data collected from two runs of the flywheel. Fig.6 shows synchronous displacements with and without UFRC. The data for UFRC Off only goes to 15,000 rpm because the dynamic current tends to start increasing significantly beyond that point. The data for UFRC On, shows low synchronous vibration up to the over speed operating point of 37,000 rpm. In this case, between 10,000 and 15,000 rpm the displacement is lower with UFRC On although this is not always the case. Fig. 7 shows synchronous currents with and without UFRC. Here clearly the synchronous current is lower and above

7,000 rpm it is near zero. With the synchronous current near zero, the synchronous bearing load is also near zero. This is an excellent benefit for an energy storage flywheel, because it substantially reduces housing vibration and rotor eddy current losses. Rotor eddy current losses are reduced because there is no changing flux required at the spin frequency to compensate for unbalance.

5. THERMAL MEASUREMENTS

A key requirement for an energy storage flywheel is to minimize losses, which optimizes overall system storage efficiency. This drives the choice of vacuum operation to minimize windage losses, and magnetic bearings to minimize bearing losses. Minimizing losses that generate heat on the rotor then becomes particularly critical since any heat generated on the rotor must be radiated to the housing. This is because there is no mechanical contact and thus no convection or conduction path from rotor to housing. For this reason, the bearing and motor design must concentrate on minimizing rotor eddy current losses. Further, it is important to predict and measure the steady state rotor temperature, to ensure that a reasonable rotor temperature can be maintained. Desired target rotor temperature is 125°C, but the existing design is acceptable up to 150°C.

To this end, a series of long term tests under realistic operating conditions are planned to validate steady-state rotor temperature. Analytical estimates of rotor losses and radiation heat transfer were also made to assess the reasonableness of the data and to guide future more detailed analysis and testing.

5.1 Rotor Temperature versus Time Measurements

The initial test performed is a 35 hour run at a constant 36,000 rpm. The motor was at idle, supplying just enough current to maintain the desired speed. The idle condition is a good initial test condition for this flywheel since it is designed to idle at 36,000 rpm for long periods with short bursts of power generation. Fig. 8 shows a plot of the rotor temperature versus time during the test. The rotor temperature is approaching a steady state temperature of 98°C, a 67°C rise from the starting temperature of 31°C. This is well below the design target of 125°C and is a very comfortable temperature for a steel rotor. Additional testing underway now will measure temperature rise using a number of charge/discharge cycles. The data can be well fitted by an exponential curve,

$$T = T_{final} - (T_{final} - T_{start})\, e^{(-t/\tau)} \qquad \textbf{(3)}$$

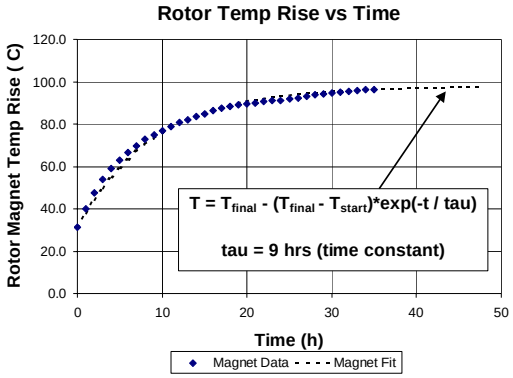

Fig. 8 Rotor temperature rise with time at maximum speed.

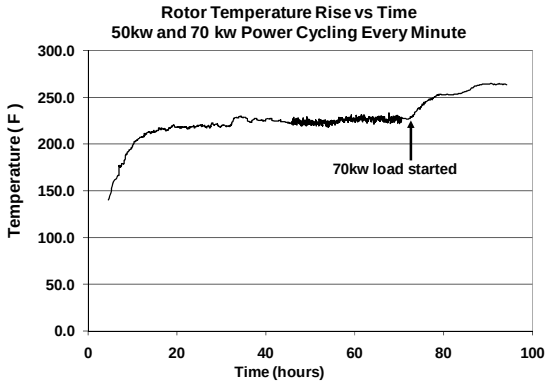

Fig. 9 Rotor temperature rise during 50kw and 70kw cycling every minute at 10,000 rpm to 18,000 rpm.

where T is temperature, the subscripts *start* and *final* are the initial and steady-state temperatures respectively, t is time from the start, and τ is a time constant. As shown in Fig. 8, a time constant of 9 hours provides a good fit to the data. The expression in equation (A) is typical of systems that can be modeled as lumped systems with heat generation (a ball bearing temperature transient is another example).

Additional testing under high cycling conditions at reduced power and speed resulted in the magnet temperature rise shown in Fig. 9. As seen, cycling from 10,000 rpm to 18,000 rpm every minute at 50kw brought the magnet temperature to 107°C (225°F). Increasing power to 70 kw increased magnet temperature to 129°C (264°F). While high power frequent cycling increases rotor temperature, reduction in operating speed can offset the increased rotor heating to allow high cycling operation of the flywheel.

6. CONCLUSIONS

The development of an industrial energy storage flywheel module was described. A gain scheduled control strategy used for the magnetic bearings was discussed and response results presented. Synchronous response measurements showed the benefits of adaptive synchronous cancellation for reducing dynamic current and load. Preliminary rotor temperature versus time measurements show that the flywheel rotor steady state temperatures are under 100°C when idling at 36,000 rpm, well below the design target. Future planned thermal testing will characterize the temperature rise for various other loading scenarios.

REFERENCES

[1] McMullen,P., Hawkins, L., Huynh, C., Dang, D., "Design and Development of a 100 kW Energy Storage Flywheel for UPS and Power Conditioning Applications", *Proc. of PCIM*, Nuremburg, Germany, May, (2003).

[2] Hayes, R.J., Kajs, J.P., Thompson, R.C., Beno, J.H., "Design and Testing of a Flywheel Battery for a Transit Bus", SAE 1999-01-1159, (1998).

[3] Hawkins, L.A., Murphy, B.T., Kajs, J.P., Analysis and Testing of a Magnetic Bearing Energy Storage Flywheel with Gain-Scheduled, MIMO Control, *ASME 2000-GT-405, Presented at ASME IGTI Conference*, Munich, Germany, May 8-11,(2000)

[4] Hawkins, L., Murphy, B., Zierer, J., Hayes, R., "Shock and Vibration Testing of an AMB Supported Energy Storage Flywheel", *Proc. of 8th Intl. Symposium on Magnetic Bearings, Mito, Japan, August*, (2002).

[5] McMullen, P., Huynh, C., Hayes, R., "Combination Radial-Axial Magnetic Bearing", *Proc. of 7th Intl. Symposium on Magnetic Bearings, Zurich, Switzerland*, August, (2000).

[6] Hawkins, L.A., McMullen, P.M., Vuong, V., "Development and Testing of the Backup Bearing System for an AMB Energy Storage Flywheel", *ASME GT2007-28290, Presented at ASME IGTI Conference*, Montreal, Canada, May 14-17, (2007).

[7] Ankowiak, B.M., Nelson, F.C., "Rotordynamic Modeling of An Actively Controlled Magnetic Bearing Gas Turbine Engine", *ASME 97-GT-13, 1997 IGTI Turbo-Expo*, Orlando, June, (1997).

[8] Knospe, C. R., Tamer, S.M., "Experiments in Robust Unbalance Response Control," *Proc. 5th Intl. Symp. on Magnetic Bearings, Kanazawa, Japan*, August, (1996).

[9] R. Herzog, Ph. Bühler, C. Gähler and R. Larsonneur: "Unbalance Compensation Using Generalized Notch Filters in the Multivariable Feedback of Magnetic Bearings", *IEEE Transactions on Control Systems Technology*, Vol. 4, No. 5, Sept. (1996).